Supporting information for: Contributions of benthic microalgal biofilms to sediment organic carbon stocks across a salt marsh gradient

Graham J C Underwood[1*]

Nicola J. D. Slee[1]

Jessica C. J. Underwood[2]

Christopher I. D. Underwood[3]

James L. Pinckney[4]

[1]School of Life Sciences, University of Essex, Colchester, Essex, U.K. CO4 3SQ

[2]School of Archaeology, Geography and Environmental Science, University of Reading, Reading, U.K. RG6 6AX.

[3] Independent Scientist, Bristol. 29 Kensington Rd, BS5 7NB, U.K.

[4]Estuarine Ecology Laboratory, Department of Biological Sciences, and School of the Earth, Ocean, and Environment, University of South Carolina, Columbia, SC 29208, USA

*Corresponding Author. Graham J C Underwood, gjcu@essex.ac.uk

Supplementary methods

Benthic microalgal pigment, carbohydrate and total organic carbon concentrations.

Chemosystematic photosynthetic pigment concentrations were determined for a subset of samples collected in 2018 using high-performance liquid chromatography (HPLC) (Higgins et al., 2011). Sediment samples were lyophilized and extracted in 90% acetone (1 mL) for 18–20 h at -20 °C. The synthetic carotenoid β-apo-8'-carotenal (Sigma) was used as an internal standard. A Shimadzu 2050 HPLC equipped with a monomeric (Rainin Microsorb–MV, 0.46 x 10 cm, 3 μm) and a polymeric (Vydac 201TP54, 0.46 x 25 cm, 5 μm) reverse-phase C18 column in series was the stationary phase. The mobile phase was a nonlinear binary gradient of 80% methanol and 20% 0.50 M ammonium acetate, and 80% methanol and 20% acetone (Pinckney et al., 2001). A photodiode array detector (PDA) was used to obtain absorption spectra and chromatogram peak areas (440 ± 4 nm). Pigment peaks were identified by comparing retention times and absorption spectra with those of pure carotenal and Chlorophyll standards (DHI, Denmark). ChemTax (version 1.95) was used to estimate the relative concentrations of major algal groups (e.g., diatoms, cyanobacteria, green algae) based on measured photopigment concentrations (Pinckney et al, 2001; Higgins et al, 2011). The matrix randomization procedure (60 simulations, Higgins et al. 2011) was applied to the initial ratio matrix derived from Lewitus et al. (2005).

Sediment total and colloidal carbohydrate concentrations were determined on subsamples of freeze-dried sediments (between 100 – 200 mg for colloidal, 10 mg for total carbohydrate), using the phenol sulphuric acid assay with a glucose standard (Dubois et al. 1956), with a modification in that samples were maintained at 100 °C after the reaction step to ensure

maximum hydrolysis of polysaccharides and complex carbohydrates (Aslam et al. 2012). Colloidal carbohydrates were extracted using a 1-hour extraction time at a salinity of 25 and 25 °C, followed by centrifugation at 3,000 g for 15 minutes (Bellinger et al. 2005; Hanlon et al., 2006). Values were calculated as µg glucose equivalents g^{-1} freeze-dried sediment.

Freeze-dried sediment samples from 2023 were measured for total carbon (TC), total inorganic carbon (TIC), and total organic carbon (TOC) on a Skalar Primacsmcs model 2MC10900 coupled to a FormacsHT model 2CA16910-02 carbon analyzer (Skalar Analytical B.V., Beda, NL). Homogenized samples were passed through a 2 mm sieve and placed in pretreated (550°C for 3-5 hours) quartz crucibles, heated to 1000 °C in the presence of a catalyst (cobalt oxide), and CO_2 liberated (total carbon) measured at 4.2 µm by IR detection and recalculated to TC content according to the calibration standard. TIC in parallel samples was converted to CO_2 by adding concentrated phosphoric acid. TOC was calculated by TOC = TC - TIC, and values expressed as % w/w content.

Near infrared Spectroscopy (NIR)

Near-infrared (NIR) spectroscopy was conducted on the 2023 dried sediment samples using an approach similar to Yang (2020). Freeze-dried sediment samples were ground to ensure homogeneity and spread in Petri dishes resting on a white surface. The measuring window of a NeoSpectra™ hand-held spectrometer (Si-Ware, Menlo Park, CA, USA) was placed on the sample, ensuring full contact between the sediment surface and the measuring window, and scans taken across the spectral wavelength range of 1,300–2,500 nm, with a resolution of 16 nm, over a 10-second scan under low-light conditions (100 µmol photons m^{-2} s^{-1}). All scans were

calibrated using the Neo-Spectra reference calibration plate provided. Samples with insufficient sediment material to ensure this coverage were omitted.

NIR spectral data (wavelengths in nm against reflectance percentages, Figure S6ab) for the sediments were used in a Principal Components Analysis (PCA) to determine differences between habitat types. The PCA was conducted on spectra pretreated with the Savitzky-Golay (SG) smoothing filter (window size = 11, first order derivative), a standard approach to emphasise peaks in NIR spectral data (Yang 2020; Walden et al. 2024). Principal components 1 and 2 sample scores from the SG-PCA were used in regression analyses to determine how NIR spectra corresponded to biofilm properties and organic carbon contents across the different habitat types.

Modelling approaches

The spatial distribution of four different habitat types (USM, SpS, SpT, MF) across the North Inlet Estuary was mapped (Fig. 1) based on LIDAR data and the relationship between the distribution of habitats across the tidal frame (North American Vertical. Data 1988) from low to high water. The upper and lower tidal height bounds for the USM, SpS, SpT, and MF habitat types were determined from the sample heights from the 2018 and 2023 data (Figure S6A) and information from Morris et al. (2005). The NOAA tidal height data were directly comparable with detailed ROV and LIDAR of tidal elevations and habitat types of the NIE by Wang et al. (2023), with a mean difference of ± 0.06m. Using lm() and poly() functions in R, polynomial curve fitting determined the relationship between sediment %TOC and tidal elevation (Equation 1), and sediment bulk density and tidal elevation (Equation 2). Sediment bulk density varied with habitat type (Figs. S2a, S3e, Kruskal-Wallis $\chi^2 = 106.25$, df = 5, $p < 0.001$) and there was a

significant polynomial relationship between sediment bulk density and tidal height (r^2 = 65.6%, excluding ChM and ChS habitats). The best fit was determined by comparing polynomial models with ANOVA.

[Equation 1]

%TOC = - 0.603*(tidal height)^3 - 2.456*(tidal height)^2 - 2.114*(tidal height) + 4.055

where (tidal height) is NOAA tidal height in metres. r^2 = 73.0

[Equation 2]

Sediment bulk density=1.5938*(tidal height)^4 + 0.5042*(tidal height)^3 + 1.2838*(tidal height)^2 + 0.11686*(tidal height) + 0.1356. r^2 = 65.6

where (tidal height) is NOAA tidal height in metres.

Using the relationships between %TOC and tidal height (Equation 1) and corresponding sediment bulk density values (Equation 2) and the distribution of habitat zones within the tidal height range, the sediment TOC stocks (g C m^{-2} to a depth of 10 cm) across the NIE was derived from the NOAA height data, using the "Raster Calculator" in QGIS. TOC was estimated in the top 10 cm of sediment, based on the relatively even profiles of total carbohydrate (Figure 2) and %LOI to that depth. Each pixel was categorized into a habitat type based on its tidal height. Areal values of TOC (per hectare, ha^{-1}) were determined by overlaying a grid of 100m x 100m squares across the NIE site, summing the individual habitat pixel values ha^{-1} to obtain an integrated TOC stock per hectare capturing habitat heterogeneity. The mean number of pixels was 8,886, the median was 10,087, and the maximum count was 10,094 pixels. This model was applied to tidal heights in the range of -0.785 to 0.981 m above the vertical datum (NAVD 88:

North American Vertical Datum of 1988), which captured most of the salt marsh habitat (Morris et al. 2005). Pixels with a height outside of this range received a 'null' value. Hence, hectare grids placed around the main water channels have many null values and hence a lower averaged carbon stock. This allowed us to model TOC stocks for individual habitats at a scale of approximately 1 m^2 and capture the heterogeneity of the marsh at m^2 and ha spatial scales.

The contribution of BMA-organic carbon to total sediment organic carbon stock was estimated from the measured contributions of colloidal carbohydrates to %TOC in different habitats (Table 1), literature values of the proportions of extracellular and intracellular carbon produced by cultured estuarine benthic diatoms (Smith and Underwood 2000; Aslam et al. 2012) and cell carbohydrate : protein: lipid ratios, and relationships between total carbohydrate, protein, and lipid content of microalgae (Courtois de Viçose et al. 2012) (Equation 3). These factors were combined with the Total Organic carbon model to field measurements for each habitat type to obtain concentrations of BMA total organic carbon (g BMA TOC m^{-2} to a depth of 2.5 cm) across the NEI. A depth of 2.5 cm was chosen for determining BMA TOC stock, based on the profile data for Chl *a* and colloidal carbohydrate (Figure 2).

[Equation 3].

BMA TOC stock 25mm = sediment TOC in 5 mm (Equ.1 and 2) * habitat value for percent TOC from colloidal carbo. (Table 1) / 0.544 (ratio of colloidal to total carbohydrate in BMA[1]) then / 0.47 (ratio of ratios of carbohydrate, protein, lipids in cells[2]), multiply sum * 5 (to allow for 2.5 cm depth)

[1]Smith and Underwood, 2000; Aslam et al., 2012; [2]Courtois de Viçose, et al., 2012.

Supplementary results

Table S1. Sample dates, site names and codes, site elevation and codes, sample size and habitat types sampled in 2018 and 2023 in the North Inlet Estuary, South Caroline, USA (see Figure 1).

Habitat type[1]	Site code	Site name	Elevation (m) mean ± st.dev.	Sample size	Sampling date
USM	CLS	Clambank sand	0.59 ± 0.02	10	26/07/2018
SpS	CSP	Clambank short *Sporobolus*	0.54 ± 0.03	10	26/07/2018
ChS	DSD	Debidue sand flat	-0.47 ± 0.02	10	27/07/2018
ChM	DNM	Debidue new mudflat	-0.21 ± 0.04	10	27/07/2018
MF	BBC	Bread and Butter Creek	-0.59 ± 0.14	10	28/07/2018
MF	OLC18	Oyster Landing mudflat	-0.21 ± 0.11	40	02/08/2018
USM	LPS	Lonesome Pine flat	0.78 ± 0.05	19	23/02/2023
MF	OLC23	Oyster Landing mudflat	-0.24 ± 0.29	19	25/02/2023
SpS	OSP	Oyster Landing short *Sporobolus*	0.43 ± 0.02	19	26/02/2023
SpT	MSP	Marsh boardwalk tall *Sporobolus*	0.19 ± 0.17	19	27/02/2023
USM	MBS	Marsh boardwalk_upper flat	0.80 ± 0.02	19	27/02/2023

[1]USM, upper salt marsh; SpS, short *Sporobolus*; SpT, tall *Sporobolus*; MF, mudflat; ChS, main channel sand; ChM, main channel mud

Table S2. Environmental varables (average, stan. deviation) during the two periods of study. Data (8 days prior to, and including the period of field work) obtained from NERR programme monitoring stations (see Fig. 1) at Oyster Landing (2018, 2023), Clambank (2018) and Debidue Creek (2018), from https://northinlet.sc.edu/environmental-monitoring/ , na = data not available

Variable	**year**	**n =**	**Oyster Landing**	**Clambank**	**Debidue Creek**
Air temp. (°C)	2018	1151	26.7 (1.96)	na	na
	2023	864	16.8 (4.83)		
Rainfall (mm per 15 min)	2018	1151	0.224 (1.3)	na	na
	2023	864	0.001 (0.014)		
Water temp. (°C)	2018	1151	28.4 (1.39)	28.7 (0.88)	28.3 (1.01)
	2023	864	16.8 (2.50)	na	na
Salinity	2018	1151	20.9 (8.9)	30.0 (3.26)	19.3 (9.49)
	2023	864	31.4 (2.09)	na	na
% O_2 saturation	2018	1151	49.5 (17.5)	60.9 (20.27)	58.5 (16.8)
	2023	864	84.1 (15.95)	na	na
pH	2018	1151	7.16 (0.38)	7.48 (0.26)	7.34 (0.30)
	2023	864	7.68 (0.20)	na	na
PO_4^{3-} (µmol. l^{-1})	2018	7	0.37 (0.088)	0.19 (0.148)	0.24 (0.054)
	2023	6-48	0.33 (0.021)	0.28 (0.04)	0.21 (0.038)
NH_4^+ (µmol. l^{-1})	2018	7	15.09 (5.03)	7.94 (6.125)	9.13 (1.677)
	2023	6-48	2.82 (0.21)	3.34 (0.422)	3.00 (0.54)
NO_2^- (µmol. l^{-1})	2018	7	0.36 (0.075)	0.20 (0.159)	0.31 (0.047)
	2023	6-48	0.10 (0.002)	0.10 (0.004)	0.10 (0.002)
NO_3^- (µmol. l^{-1})	2018	7	0.94 (0.242)	0.68 (0.531)	1.30 (0.227)
	2023	6-48	0.26 (0.01)	0.48 (0.07)	0.29 (0.058)

Table S3. Relative taxonomic composition derived from 2018 HPLC pigment data using ChemTax. Significant differences ($p < 0.05$ or less) in relative algal taxonomic composition between sediment types for each algal group, and between significant β coefficients indicated by different superscripts^{A,B}. n.a. = not applicable. Linear regression models for predicting sediment colloidal carbohydrate concentrations, based on the equation: $\log_{10}$ ([coll. carbo.] + 1) = α + β $\log_{10}$ ([chl. a] + 1) for the complete data set (ALL) and for each sediment type. Mean ± standard error (n) of regression parameters, and significance of β value indicated. *$p < 0.05$, **$p < 0.01$, ***$p < 0.001$, ns = $p > 0.05$. Regression parameters for model of Underwood & Smith (1998) also given.

Sed. type	Relative taxonomic composition[1] (%)	α (intercept)	β (slope)	β sig.	years
ALL	n.a.	1.76 ± 0.03	0.55 ± 0.026 (180)	***	2018, 2023
USM	Diat:80.3^{A} Grn:12.6^{A}, Cyn 6.9^{A}	1.91 ± 0.03	0.27^{A} ± 0.051 (48)	***	2018, 2023
SpS	Diat:81.6 Grn:17.1, Cyn 1.3^{B}	2.10 ± 0.15	0.37^{AB} ± 0.106 (19)	***	2023
SpT	n.a.	1.76 ± 0.09	0.54^{AB} ± 0.065 (24)	***	2018, 2023
MF	Diat:77.3 Grn:17.5, Cyn 5.2^{A}	1.58 ± 0.15	0.70^{B} ± 0.102 (69)	***	2018, 2023
ChS	Diat:86.8 Grn:12.3, Cyn 0.9^{B}	1.16 ± 0.37	1.05^{BC} ± 0.356 (10)	**	2018
ChM	Diat:93.0^{B} Grn:6.2^{B}, Cyn 0.8^{B}	2.70 ± 1.71	-0.83 ± 2.270 (10)	ns	2018
Underwood & Smith (1998)		1.40 ± 0.06	1.02^{C} ± 0.045 (172)	***	

[1]Diat = diatoms, Grn = includes chlorophytes, euglenophytes, Cyn = cyanobacteria..

Figure S1. Example habitats in the North Inlet Estuary (NIE), South Carolina, U.S.A., sampled in this study; (a) upper salt marsh (USM) habitat, with stands of short *Sporobolus* (SpS) in the background , site LPS; (b), Short *Sporobolus* habitat (SpS), site OSP; (c) minicore sampling syringes (diameter 2 cm) in short *Sporobolus* habitat (SpS), site OSP; (d) tall *Sporobolus* habitat (SpT), with adjacent mudflat, site OSP; (e) mudflat habitat (MF) with tall *Sporobolus* habitat (SpT), site BBC; (d) main channel mudflat (ChM), site DNM. For Site codes, see Table 1. (photographs, a, b, c, taken in Feb. 2023; d, e, f, taken in July 2018).

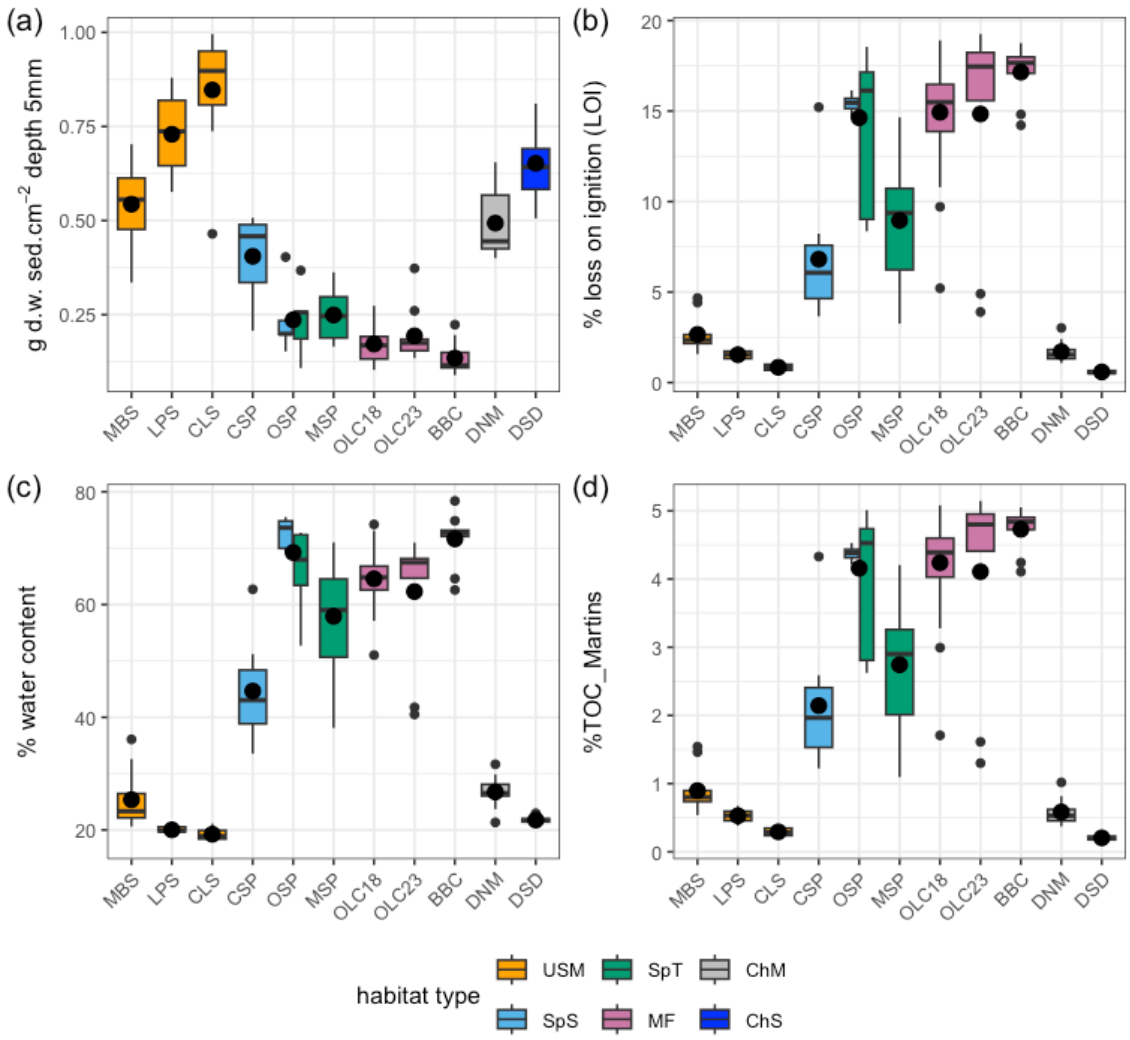

Figure S2. Boxplots of (a) sediment bulk density (g dry weight of sediment cm^{-2}, depth 5 mm); (b) sediment organic matter (% loss on ignition, LOI); (c) sediment % water content; (d) derived %TOC - model Martins et al. (2022), in the top 5 mm of sediment in 11 sites in the North Inlet Estuary, SC, in 2018 and 2023 (mean values indicated by point).

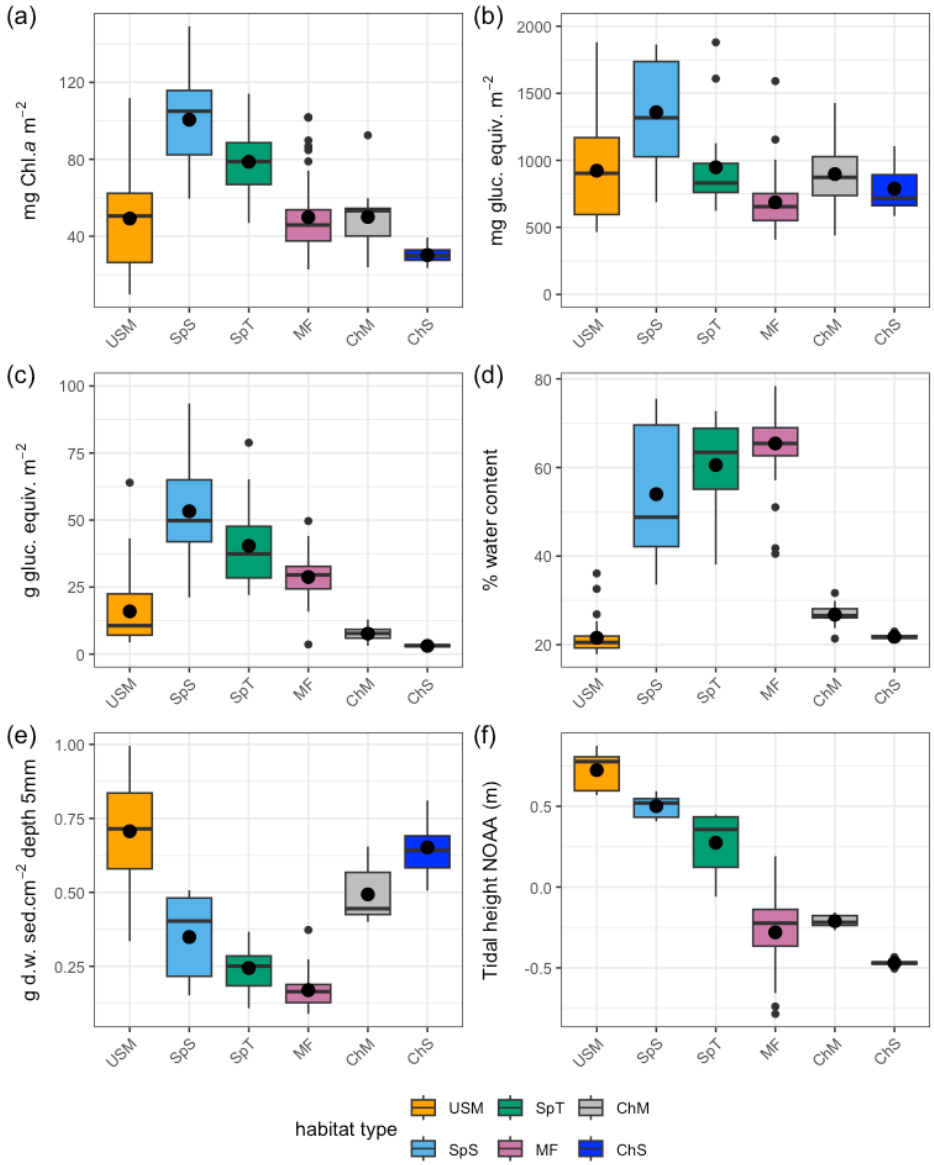

167 **Figure S3.** Boxplots of areal values (m^{-2}, to a depth of 5 mm) of (a) sediment Chl *a*; (b)
168 colloidal carbohydrates, and (c) total carbohydrates; (d) sediment % water content, and (e)
169 sediment bulk density, (f) height in the tidal range (North American Vertical Datum 1988), for
170 each habitat type sampled in the in the North Inlet Estuary in 2018 and 2023 (mean values
171 indicated by point).

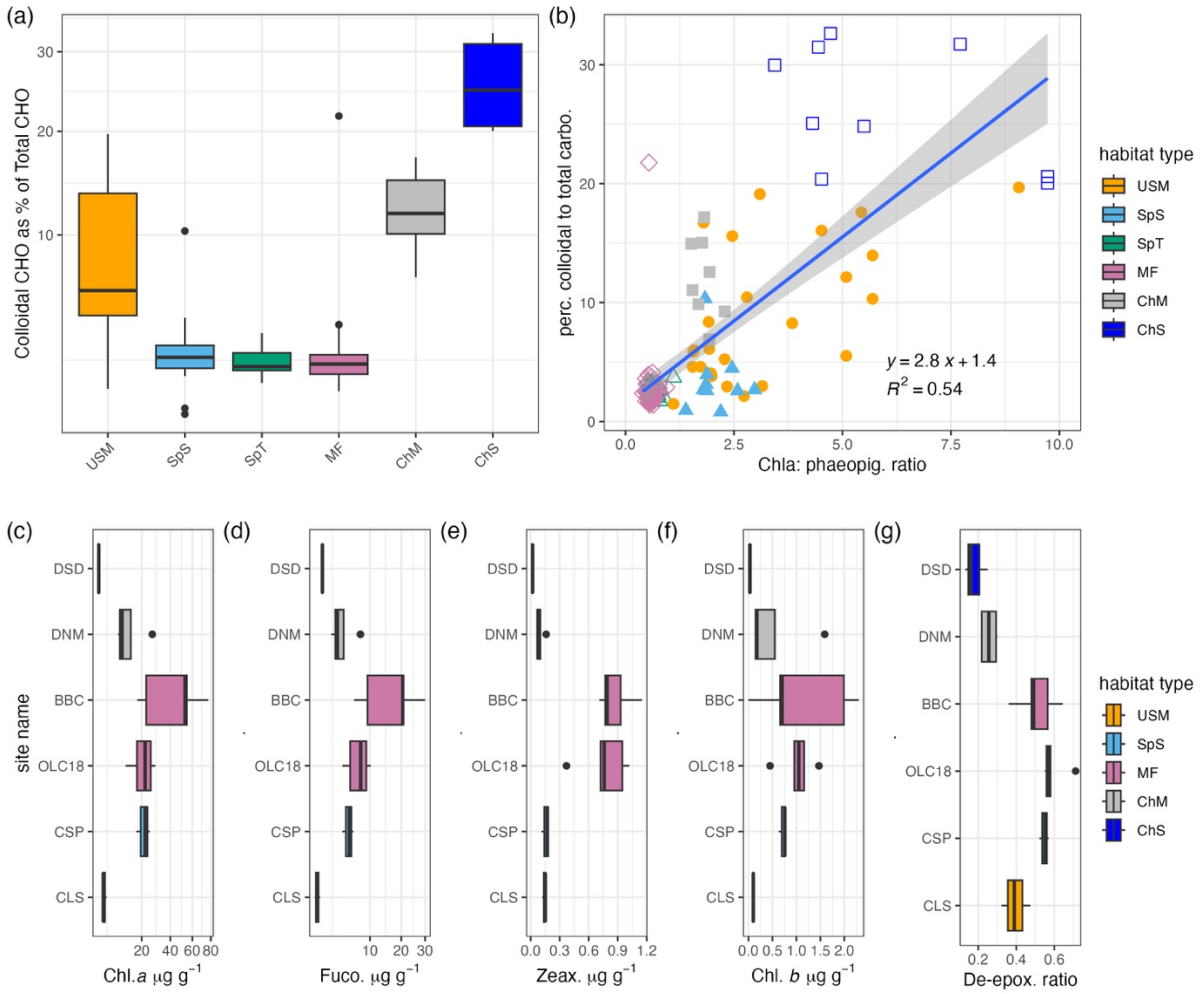

172

173 **Figure. S4**. (a) Boxplot of contribution of colloidal carbohydrate to total carbohydrate (% of
174 total), (b) the relationship between the colloidal contribution to total carbohydrate (%) and Chl. *a*
175 : phaeopigment ratios (spectrophotometry) in biofilms across the NIE sampled in 2018 and 2023.
176 (d-f) boxplots of total chlorophyll *a* + Chl *a* isomers, Fucoxanthin, Zeaxanthin and chlorophyll *b*
177 content (measured by HPLC) and (g) de-epoxidation ratios (Diatoxanthin / (Diatoxanthin+
178 Diadinoxanthin) content) in the top 5 mm of sediment from sites sampled in 2018.

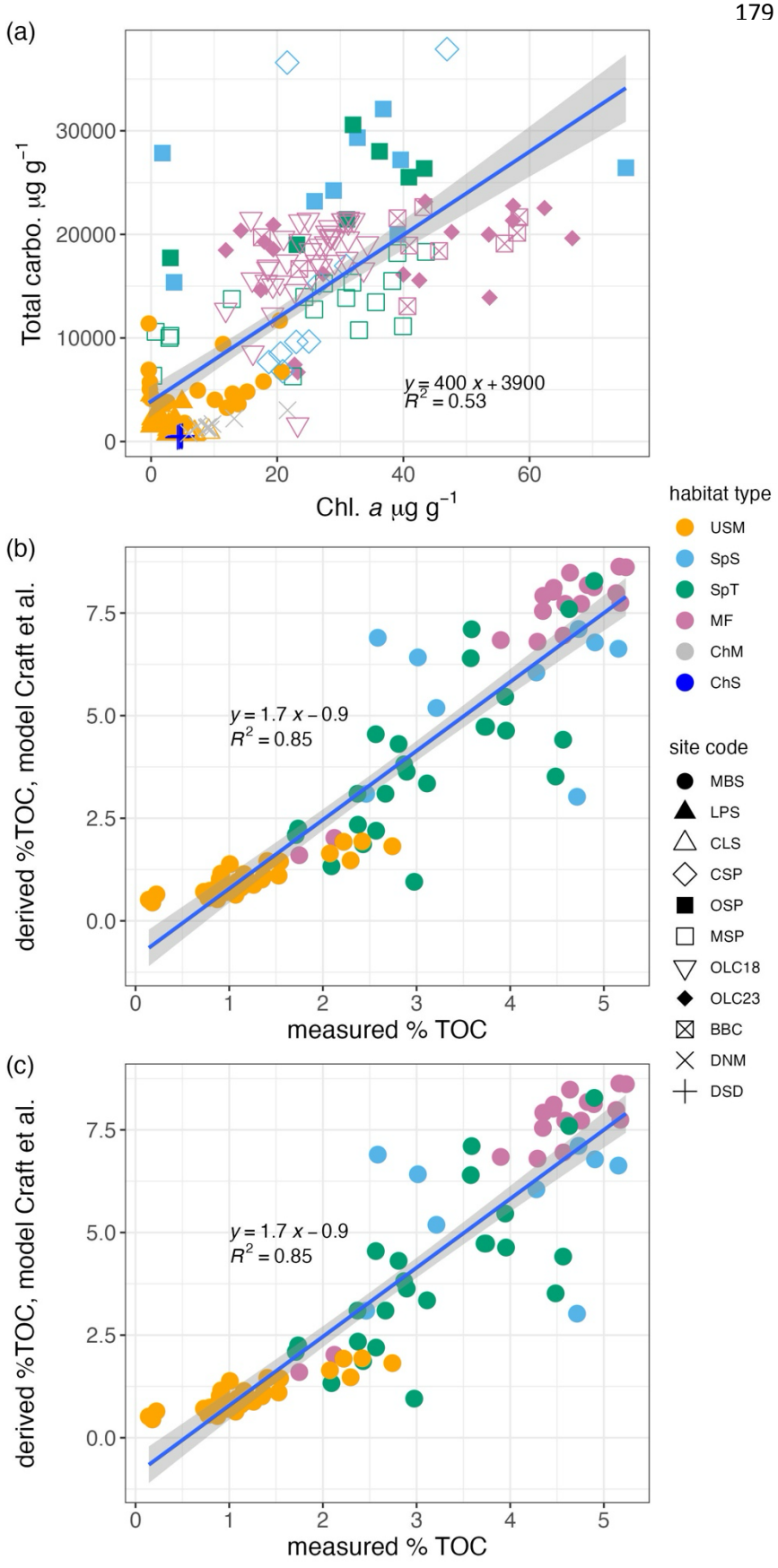

Figure S5. (a) Relationship between sediment Chl. *a* and sediment total carbohydrate content (µg g^{-1}) across all sites and habitat types in the top 5 mm of sediment in North Inlet Estuary, S.C., in 2018 and 2023. (b) Relationship between derived %TOC values from Craft et al. (1991) and (c) Maxwell et al. (2023) models with direct measures of %TOC in the top 5 mm of sediment from samples taken in 2023.

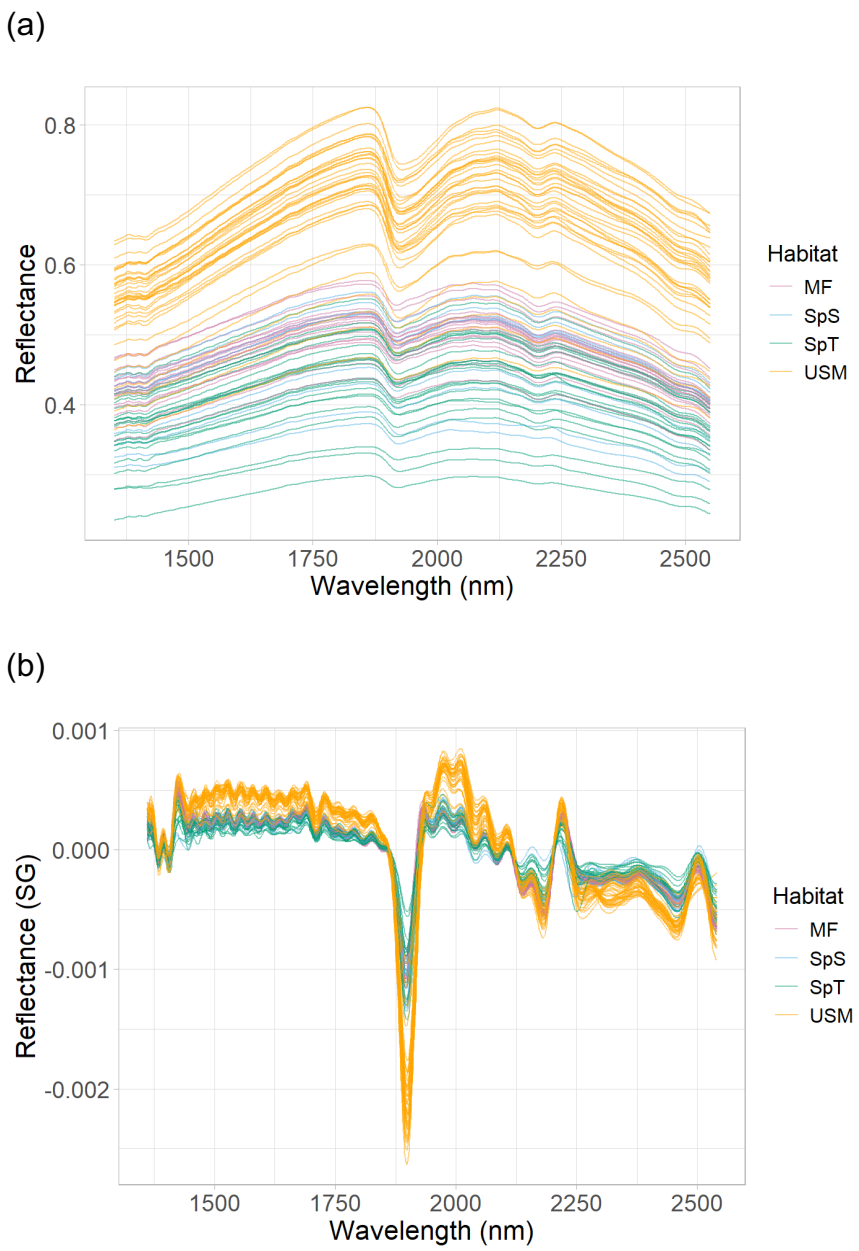

199

200 **Figure S6** (a), Individual spectral scans (NIR reflectance) for sediment samples from four
201 different habitat types in the North Inlet Estuary, South Carolina, sampled in February 2023. (b)
202 Individual spectra transformed using 1st order derivative Savitzky Golay-smoothing. These data
203 were used in the PCA (see Fig. 4a).

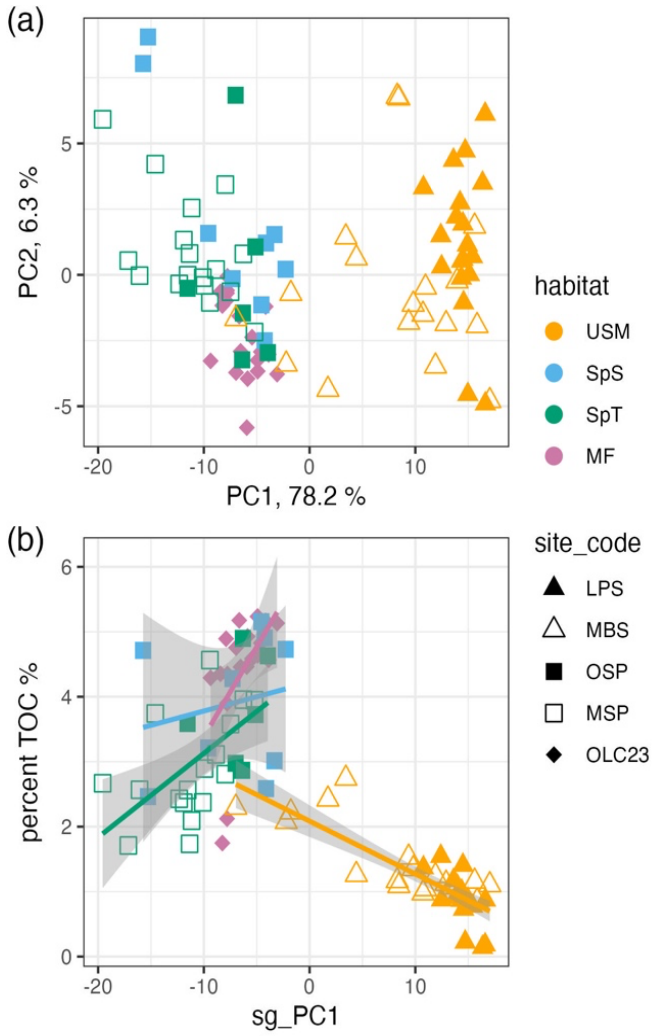

204

205 **Figure S7** (a) Principal Components 1 and 2 (explaining 83.5% of the variance) from PCA of
206 Savitzky Golay-smoothed NIR spectra for dried sediments from 2023; (b) relationship between
207 PCA component 1 scores (PC1) of NIR scan data and %TOC for sediment samples from four
208 habitats from North Inlet Estuary, S.C. sampled in 2023 (regression lines and 95% confidence
209 limits shown for each habitat type).

210

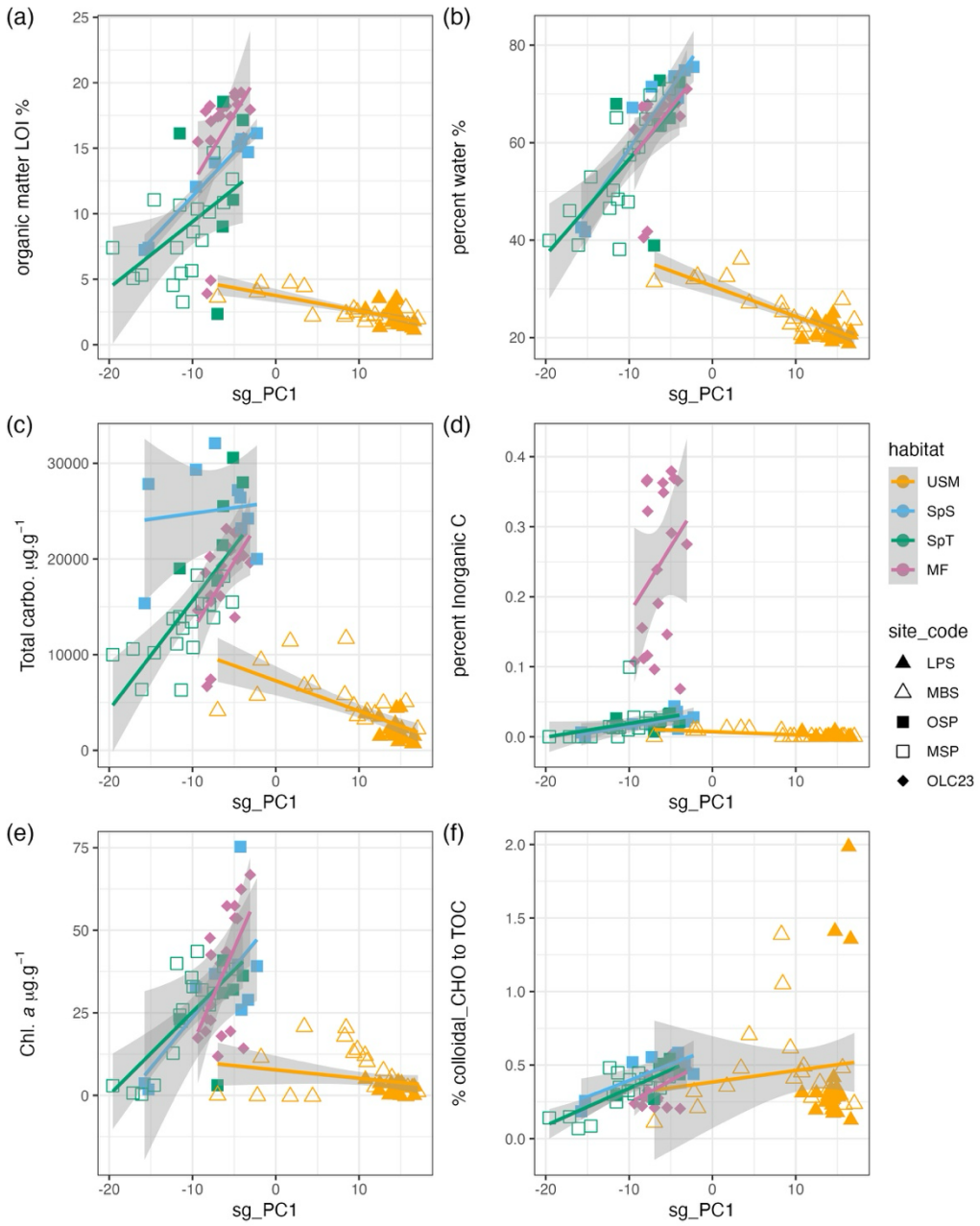

211 **Figure S8** (a-f). Relationships between Principal Component Analysis component 1 scores
212 (PC1) of NIR scan data for sediment samples from 2023, coded by habitat and (a) sediment
213 organic matter (%LOI); (b) %water content; (c) sediment total carbohydrate; (d) percent total
214 inorganic carbon; (e) sediment Chl *a*; (f) % contribution of colloidal carbohydrate to TOC.
215 Individual regression lines (with 95% confidence limits) for each habitat type shown.

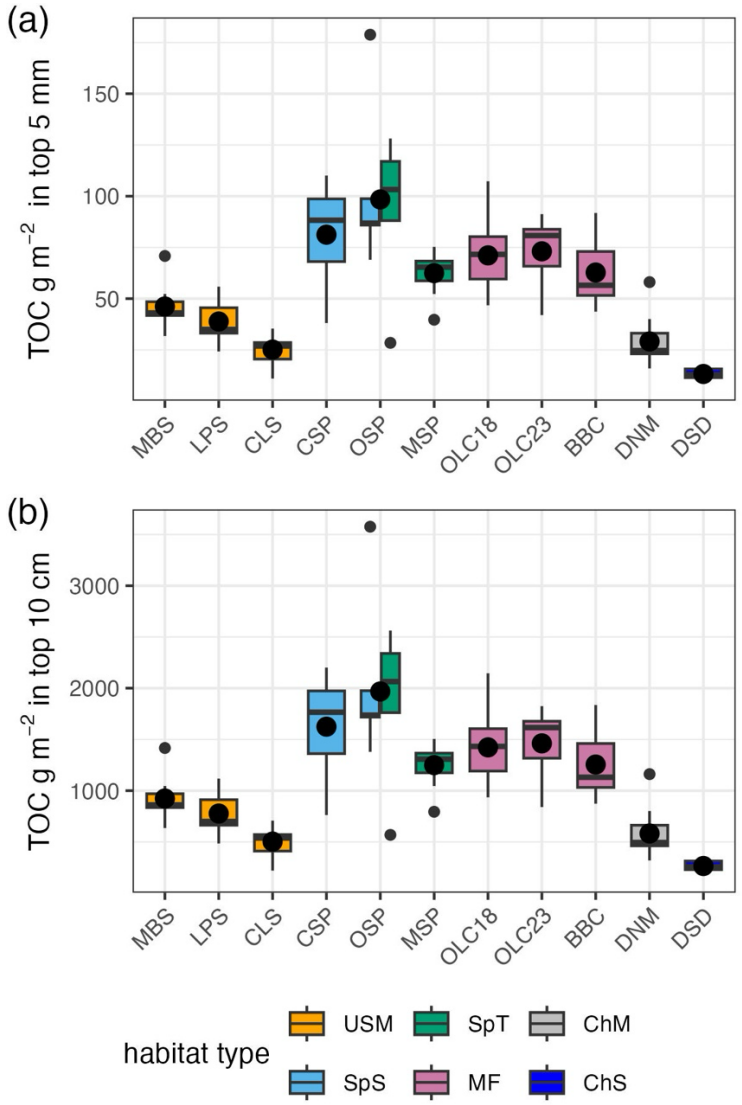

Figure S9. Boxplots of sediment Total Organic Carbon stock (g C m^{-2}) in (a) the top 5 mm sediment and (b) scaled to the top 10 cm depth of sediment, at different sites in the North Inlet Estuary, South Carolina, U.S.A. (mean values indicated by point).

Supplementary references

Aslam, S. N., Cresswell-Maynard, T., Thomas, D. N., and Underwood, G. J. C. 2012. Production and characterisation of the intra- and extracellular carbohydrates and polymeric substances (EPS) of three sea ice diatom species, and evidence for a cryoprotective role for EPS. *Journal of Phycology* 48: 1494–1509.

Courtois de Viçose, G., Porta, A., Viera, M. P., Fernández-Palacios H., Izquierdo, M. S. 2012. Effects of density on growth rates of four benthic diatoms and variations in biochemical composition associated with growth phase. *Journal of Applied Phycology* 24: 1427-1437.

Dubois, M., Gilles, K. A., Hamilton, J. K., Rebers, P. A., and Smith, F. 1956. Colorimetric method for determination of sugars and related substances. *Analytical Chemistry* 28: 350-56.

Hanlon, A. R. M., Bellinger, B., Haynes, K., et al. 2006. Dynamics of extracellular polymeric substance (EPS) production and loss in an estuarine, diatom-dominated, microalgal biofilm over a tidal emersion-immersion period. *Limnology and Oceanography* 51: 79–93.

Lewitus, A., White, D., Tymowski, R., Geesey, M., Hymel, S., and Noble, P. 2005. Adapting the CHEMTAX method for assessing phytoplankton taxonomic composition in Southeastern U.S. estuaries. *Estuaries* 28:160-172.

Pinckney, J. L., Richardson, T. L, Millie, D. F., and Paerl, H. W. 2001. Application of photopigment biomarkers for quantifying microalgal community composition and in situ growth rates. *Organic Geochemistry* 32: 585-595.

241 Smith, D. J., and Underwood, G. J. C. 2000. The production of extracellular carbohydrate
242 exopolymers (EPS) by estuarine benthic diatoms: the effects of growth phase and light and dark
243 treatment. *Journal of Phycology* 36: 321-333.

244